Stability of Interrupted Cutting by Temporal Finite Element Analysis

P. V. Bayly*
Washington University, St. Louis, MO 63130

J. E. Halley
OpSource Inc., St. Louis, MO 63112

B. P. Mann
Washington University, St. Louis, MO 63130

M. A. Davies
UNC Charlotte, NC 28233

Chatter in milling and other interrupted cutting operations occurs at different combinations of speed and depth of cut from chatter in continuous cutting. Prediction of stability in interrupted cutting is complicated by two facts: (1) the equation of motion when cutting is not the same as the equation when the tool is free; (2) no exact analytical solution is known when the tool is in the cut. These problems are overcome by matching the free response with an approximate solution that is valid while the tool is cutting. An approximate solution, not restricted to small times in the cut, is obtained by the application of finite elements in time. The complete, combined solution is cast in the form of a discrete map that relates position and velocity at the beginning and end of each element to the corresponding values one period earlier. The eigenvalues of the linearized map are used to determine stability. This method can be used to predict stability for arbitrary times in the cut; the current method is applicable only to a single degree of freedom. Predictions of stability for a 1-degree of freedom case are confirmed by experiment.
[DOI: 10.1115/1.1556860]

1 Introduction

Control of chatter in milling is of great importance to manufacturers. Chatter is a dynamic instability caused by "regeneration of waviness." Koenigsberger and Tlusty [1] and Tobias [2] developed models of chatter in the form of delay-differential equations that were analyzed in the frequency domain. Stability predictions from these analyses are approximate in the case of milling, or interrupted turning, since they rely on the fundamental assumption of continuous cutting.

In milling, cutting is interrupted: each tooth enters and leaves the work piece (Fig. 1). While in the cut, force is related to tool displacement. When out of the cut, force is not dependent on tool displacement. In effect, the coefficients that relate displacement to cutting force change from zero (when the tool is free) to large numbers (when the tool is cutting). While it is not difficult to incorporate such effective variation of coefficients into time-domain simulation [3], it is very inefficient to use time-marching numerical simulation to explore parameter space. Altintas and Budak [4], Davies et al. [5,6], Corpus and Endres [7], and Insperger and Stepan [8] have proposed analytical methods that explicitly account for the interrupted nature of milling. These authors have generated stability diagrams analogous to the classical "lobes" obtained by Tlusty, Tobias, and their co-workers [1,2]. Corpus and Endres [7] capture the intermittency by including many harmonics in the Fourier series of the time-varying coefficients. This approach loses accuracy as the relative time in the cut decreases.

Davies et al. [5,6] examine the limit in which the time in the cut is infinitesimal. The cutting process is modeled as an impulse, the magnitude of which is proportional to amount of material removed. By matching successive "impulse responses" Davies et al. obtain a discrete representation of the system (a map). The stability properties off the map are then investigated analytically. Bayly et al. [9] extend this work by considering short, but not infinitesimally short, time in the cut. The equation of motion during cutting was analyzed by the method of weighted residuals ([10,11]).

The work of Davies et al. [5,6] and Bayly et al. [9] loses accuracy as the time in the cut becomes longer. To look at longer times in the cut, Insperger and Stepan [12] derive an approximate expression for the time delay in the form of an integral, obtain a large (120×120, e.g.) time-periodic matrix differential equation, and use Floquet theory to determine stability boundaries.

In this paper we describe an alternative analysis of interrupted cutting with arbitrary time in the cut. The method is based on the use of multiple finite elements in the time domain. Position and velocity are matched at the beginning and end of each element. The regenerative cutting force depends on values of the displacement one period earlier, and a discrete version of the system is obtained. The eigenvalues of the linear map determine its stability. This method is used to explore the effects of speed, depth of cut, and time in the cut for 1-DOF cutting. Experimental evidence is presented to confirm stability predictions.

2 Model and Analysis

A generic model of interrupted turning is shown in Fig. 1. Davies et al. [5,6] showed that this model also approximates very low radial immersion milling. In this model the system is governed by two different equations of motion; the equation to be used depends on whether the tool is in contact with the work piece. Either the tool or the work piece can move; the other is assumed rigid.

2.1 Free Vibration. When the tool is not in contact with the work piece, the equation of motion is:

$$m\ddot{x}+c\dot{x}+kx=0 \tag{1}$$

which has the solution $x(t)=c_1e^{\lambda_1 t}+c_2e^{\lambda_2 t}$ where $\lambda_{1,2}=-\xi\omega_n \pm i\omega_d$. If we let $t=t_c$ as the tool leaves the material (the position shown in Fig. 1), we find a state transition matrix is obtained that relates the final state of free vibration to the initial state:

$$\begin{Bmatrix} x(t_f+t_c) \\ \nu(t_f+t_c) \end{Bmatrix} = \frac{1}{\lambda_1-\lambda_2}\begin{bmatrix} \lambda_1e^{\lambda_2 t_f}-\lambda_2e^{\lambda_1 t_f} & e^{\lambda_1 t_f}-e^{\lambda_2 t_f} \\ \lambda_1\lambda_2e^{\lambda_2 t_f}-\lambda_1\lambda_2e^{\lambda_1 t_f} & \lambda_1e^{\lambda_1 t_f}-\lambda_2e^{\lambda_2 t_f} \end{bmatrix} \times \begin{Bmatrix} x(t_c) \\ \nu(t_c) \end{Bmatrix} \tag{2}$$

This equation is true for every period, so that for all n:

$$\begin{Bmatrix} x(nT) \\ \nu(nT) \end{Bmatrix} = [M]\begin{Bmatrix} x((n-1)T+t_c) \\ \nu((n-1)T+t_c) \end{Bmatrix}. \tag{3}$$

where M is the 2×2 matrix in Eq. (2).

*Address for correspondence: Mechanical Engineering, Box 1185 Washington University St. Louis, MO 63130 Email: pvb@me.wustl.edu

Contributed by the Manufacturing Engineering Division for publication in the JOURNAL OF MANUFACTURING SCIENCE AND ENGINEERING. Manuscript received March 2001; Revised July 2002. Associate Editor: Y. Altintas.

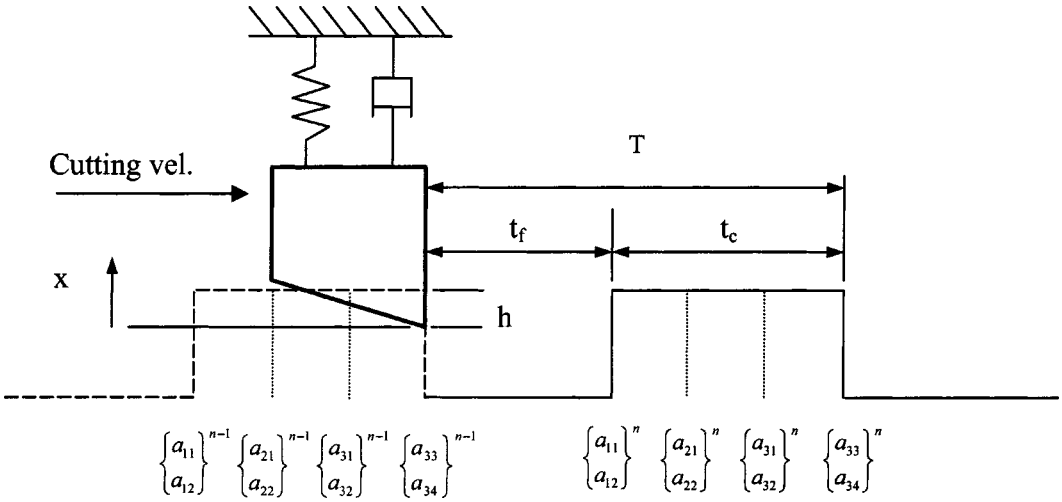

Fig. 1 Schematic diagram of the interrupted cutting process. When the tool is in contact with the work piece, the cutting force is proportional to the cross-sectional area of the uncut chip. The tool vibrates freely when not in contact with the work piece. The coefficients a_{j1} and a_{j2} specify the initial position and velocity of the tool as it enters the j^{th} element; the coefficients a_{j3} and a_{j4} specify the position and velocity of the tool at the end of the j^{th} element.

2.2 Vibration During Cutting. When the tool is in the cut, its motion is approximately governed by the linear equation

$$m\ddot{x}+c\dot{x}+kx=Cb\{h_{dc}-x+x(t-T)\} \tag{4}$$

Since this equation cannot be solved exactly, an approximate solution for the displacement of the tool during the j^{th} element of the n^{th} period of revolution is assumed in the following form [10]:

$$x(t)=\sum_{i=1}^{4} a_{ji}^{n}\phi_i(\tau(t)). \tag{5}$$

Here $\tau(t)=t-nT-\Sigma_{k=1}^{j-1}t_k$ is the "local" time within the j^{th} element of the n^{th} period, the length of the k^{th} element is t_k and the trial functions $\phi_i(\tau)$ are the cubic Hermite polynomials. On the j^{th} element these functions are:

$$\phi_1(\tau)=1-3\left(\frac{\tau}{t_j}\right)^2+2\left(\frac{\tau}{t_j}\right)^3, \tag{6a}$$

$$\phi_2(\tau)=t_j\left\{\left(\frac{\tau}{t_j}\right)-2\left(\frac{\tau}{t_j}\right)^2+\left(\frac{\tau}{t_j}\right)^3\right\}, \tag{6b}$$

$$\phi_3(\tau)=3\left(\frac{\tau}{t_j}\right)^2-2\left(\frac{\tau}{t_j}\right)^3, \tag{6c}$$

$$\phi_4(\tau)=t_j\left\{-\left(\frac{\tau}{t_j}\right)^2+\left(\frac{\tau}{t_j}\right)^3\right\}, \tag{6d}$$

These functions are only adequate for describing approximately one wavelength of periodic motion. They are defined so that their end conditions are either zero or unity [9]. Because of the special end conditions of the trial functions, the initial and final displacements and the initial and final velocities of each element can each be specified by a single coefficient:

$$\text{Initial conditions: } x(t_{0j}^{n})=a_{j1}^{n}, \quad \nu(t_{0j}^{n})=a_{j2}^{n}, \tag{7a}$$

$$\text{Final conditions: } x(t_{1j}^{n})=a_{j3}^{n}, \quad \nu(t_{1j}^{n})=a_{j4}^{n}, \tag{7b}$$

$$\text{Where: } t_{0j}^{n}=\left(nT+\sum_{k=1}^{j-1}t_k\right); \quad t_{1j}^{n}=\left(nT+\sum_{k=1}^{j}t_k\right). \tag{7c}$$

On the j^{th} element the velocity, acceleration, and time-delayed displacement are

$$\dot{x}(t)=\sum_{i=1}^{4} a_{ji}^{n}\frac{d\phi_i}{dt}, \quad \ddot{x}(t)=\sum_{i=1}^{4} a_{ji}^{n}\frac{d^2\phi_i}{dt^2},$$
$$x(t-T)=\sum_{i=1}^{4} a_{ji}^{n-1}\phi_i(\tau(t)). \tag{8}$$

The displacement and velocity of the tool at the entry into the cut are specified by the coefficients of the first two basis functions on the first element: a_{11}^{n} and a_{12}^{n}. For the remainder of the elements, the position and velocity at the end of one element are equal to the position and velocity at the beginning of the next element. For each element, two more equations are needed, in order to solve for the unknown coefficients a_{j3}^{n} and a_{j4}^{n}. For the last element, these coefficients correspond to the position and velocity of the tool as it exits the material.

Substitution of the assumed solution into the equation of motion leads to a non-zero error. In the method of weighted residuals, the error is "weighted" by a set of test functions, $\psi_p(\tau)$, $p=1,2$ and the integral of the weighted error is set to zero to obtain two more equations per element [10]. The test functions are chosen to be the simplest possible functions: $\psi_1(\tau)=1$ (constant) and $\psi_2(\tau)=\tau/t_j-1/2$ (linear). On the j^{th} element, two more equations are thus obtained.

$$\int_0^{t_j}\left\{m\left(\sum_{i=1}^{4} a_{ji}^{n}\ddot{\phi}_i\psi_p\right)+c\left(\sum_{i=1}^{4} a_{ji}^{n}\dot{\phi}_i\psi_p\right)+k\left(\sum_{i=1}^{4} a_{ji}^{n}\phi_i\psi_p\right)\right\}d\tau$$
$$-\int_0^{t_j}Cb\left\{h_{dc}\psi_p-\left(\sum_{i=1}^{4} a_{ji}^{n}\phi_i\psi_p\right)+\left(\sum_{i=1}^{4} a_{ji}^{n-1}\phi_i\psi_p\right)\right\}d\tau$$
$$=0, \quad p=1,2 \tag{9}$$

Evaluation of the definite integrals leads to two equations that are linear in the coefficients of the trial functions. These equations can be written as a single matrix equation for the j^{th} element.

$$\begin{bmatrix} N_{11} & N_{12} & N_{13} & N_{14} \\ N_{21} & N_{22} & N_{23} & N_{24} \end{bmatrix}\begin{Bmatrix} a_{j1} \\ a_{j2} \\ a_{j3} \\ a_{j4} \end{Bmatrix}^{n}=\begin{Bmatrix} C_1 \\ C_2 \end{Bmatrix}$$
$$+\begin{bmatrix} P_{11} & P_{12} & P_{13} & P_{14} \\ P_{21} & P_{22} & P_{23} & P_{24} \end{bmatrix}\begin{Bmatrix} a_{j1} \\ a_{j2} \\ a_{j3} \\ a_{j4} \end{Bmatrix}^{n-1} \tag{10}$$

where

$$N_{ip}=\int_0^{t_j}\{m\ddot{\phi}_i+c\dot{\phi}+(k+Cb)\phi_i\}\psi_p d\tau, \tag{11a}$$

$$C_p=\int_0^{t_j}Cbh_{dc}\psi_p d\tau, \tag{11b}$$

$$P_{ip}=\int_0^{t_j}Cb\phi_i\psi_p d\tau. \tag{11c}$$

While the tool is in the cut, the position and velocity at the end of one element are equal to the position and velocity at the beginning of the next element.

$$\begin{Bmatrix}a_{j1}\\a_{j2}\end{Bmatrix}^n=\begin{Bmatrix}a_{(j-1)3}\\a_{(j-1)4}\end{Bmatrix}^n. \tag{12}$$

We can also re-write Eq. (3) (the relationship between the initial and final conditions during free vibration), using the coefficients a_{ji} to specify position and velocity:

$$\begin{Bmatrix}a_{11}\\a_{12}\end{Bmatrix}^n=[M]\begin{Bmatrix}a_{E3}\\a_{E4}\end{Bmatrix}^{n-1}, \tag{13}$$

where E is the total number of finite elements in the cut.

Finally, the last three matrix equations can be rearranged to obtain the coefficients of the assumed solution in terms of the coefficients at the time of the previous tooth passage (plus a constant vector). The following expression is for the case when the number of elements, $E=3$.

$$\begin{bmatrix}\mathbf{I}&\mathbf{0}&\mathbf{0}&\mathbf{0}\\\mathbf{N_1}&\mathbf{N_2}&\mathbf{0}&\mathbf{0}\\\mathbf{0}&\mathbf{N_1}&\mathbf{N_2}&\mathbf{0}\\\mathbf{0}&\mathbf{0}&\mathbf{N_1}&\mathbf{N_2}\end{bmatrix}\begin{Bmatrix}\begin{bmatrix}a_{11}\\a_{12}\end{bmatrix}\\\begin{bmatrix}a_{21}\\a_{22}\end{bmatrix}\\\begin{bmatrix}a_{31}\\a_{32}\end{bmatrix}\\\begin{bmatrix}a_{33}\\a_{34}\end{bmatrix}\end{Bmatrix}^n=\begin{bmatrix}\mathbf{0}&\mathbf{0}&\mathbf{0}&\mathbf{M}\\\mathbf{P_1}&\mathbf{P_2}&\mathbf{0}&\mathbf{0}\\\mathbf{0}&\mathbf{P_1}&\mathbf{P_2}&\mathbf{0}\\\mathbf{0}&\mathbf{0}&\mathbf{P_1}&\mathbf{P_2}\end{bmatrix}\times\begin{Bmatrix}\begin{bmatrix}a_{11}\\a_{12}\end{bmatrix}\\\begin{bmatrix}a_{21}\\a_{22}\end{bmatrix}\\\begin{bmatrix}a_{31}\\a_{32}\end{bmatrix}\\\begin{bmatrix}a_{33}\\a_{34}\end{bmatrix}\end{Bmatrix}^{n-1}+\begin{Bmatrix}\begin{bmatrix}0\\0\end{bmatrix}\\\begin{bmatrix}C_1\\C_2\end{bmatrix}\\\begin{bmatrix}C_1\\C_2\end{bmatrix}\\\begin{bmatrix}C_1\\C_2\end{bmatrix}\end{Bmatrix} \tag{14}$$

where the sub-matrices are:

$$\mathbf{N_1}=\begin{bmatrix}N_{11}&N_{12}\\N_{21}&N_{22}\end{bmatrix}, \tag{15a}$$

$$\mathbf{N_2}=\begin{bmatrix}N_{13}&N_{14}\\N_{23}&N_{24}\end{bmatrix}, \tag{15b}$$

$$\mathbf{P_1}=\begin{bmatrix}P_{11}&P_{12}\\P_{21}&P_{22}\end{bmatrix}, \tag{15c}$$

$$\mathbf{P}_2=\begin{bmatrix}P_{13}&P_{14}\\P_{23}&P_{24}\end{bmatrix}. \tag{15d}$$

The global matrices, of dimensions $(2E+2)\times(2E+2)$, for larger numbers of elements, E, are obviously analogous.

Equation (14) describes a linear discrete dynamical system, or map that can be written as

$$\mathbf{A}\vec{a}_n=\mathbf{B}\vec{a}_{n-1}+\vec{C}. \tag{16}$$

or

$$\vec{a}_n=\mathbf{Q}\vec{a}_{n-1}+\vec{D} \tag{17}$$

The eigenvalues of the transition matrix $\mathbf{Q}=\mathbf{A}^{-1}\mathbf{B}$ determine the stability of the system. In this study, we specify the physical parameters (mass, stiffness, damping, cutting pressure). For a range of operating conditions (depth of cut, b, and speed) the transition matrix is formed and the eigenvalues are found. If the magnitude of any eigenvalue exceeds one, then the solution is unstable. The boundaries between stable and unstable cutting are then plotted as a function of speed and depth of cut. It is important to point out that the cubic polynomial approximation of the surface is expected to be accurate over less than a period of vibration. As speed is decreased or time in the cut is increased, more elements are needed.

2.3 Simulation. The stability analysis was verified by numerical simulation of the equation of motion (Eq. (4)) allowing forces to go to zero when the tool is not in the cut. Simulations were performed using a standard Euler integration scheme [12]; time steps were chosen to ensure at least 100 steps per revolution or natural vibration period, and convergence of solutions was checked by further decreasing the time step.

2.4 Experimental Validation. Milling tests were performed with an experimental flexure designed to mimic the 1-DOF system described above. A monolithic, uni-directional flexure was machined from aluminum and instrumented with a single non-contact, eddy current displacement transducer. Aluminum (7075-T6) test samples 6.00 mm thick×25 mm high×75 mm long were clamped on the flexure. Each sample was then milled at a specified axial depth of cut and spindle speed. A 0.750-inch diameter carbide end mill with a single flute was used; the second flute was ground off to remove any effects due to asymmetry or runout. Feed was held constant at 0.004 in/rev.

The stiffness of the flexure to deflections in the x-direction was specified to be approximately $k\approx 2\times 10^6$ N/m; the measured stiffness was $k=2.2\times 10^6$ N/m. The natural frequency was experimentally determined to be 146.8 Hz and the damping ratio $\zeta=0.0038$, which corresponds to very light damping. In comparison, the values of stiffness in the perpendicular y- and z-directions were more than 20 times greater, as was the stiffness of the tool. The specific cutting pressure in the x-direction (C) was determined from the rate of increase of cutting force as a function of chip load during separate cutting tests on a rigid dynamometer (Kistler Model 9255B). The estimated value was $C=2.0\times 10^8$ N/m^2.

The displacement signal was anti-alias filtered and sampled (16-bit precision, 12800 samples/sec) with SigLab 20–22a data acquisition hardware connected to a Toshiba Tecra 520 laptop computer. A periodic 1/rev pulse was obtained with the use of a laser tachometer to sense a white-black transition on the rotating tool holder. Samples of displacement were taken at the 1/rev pulse to provide a Poincaré section. A cut was determined to be stable if the 1/rev-sampled position of the tool approached a steady constant value (see [13]). This led to clear distinction of stable and unstable cuts (Fig. 3).

3 Results

3.1 Stability Boundaries. Stability boundaries based on the current analysis are plotted in Fig. 2 for various fractions of time in the cut ($\rho=t_c/T$). Instability is indicated when an eigenvalue of Eq. (19) penetrates the unit circle. Two routes to instability were predicted by Davies et al. [5,6]: (1) a negative real eigenvalue passes through $\mu=-1$; (2) a complex eigenvalue attains

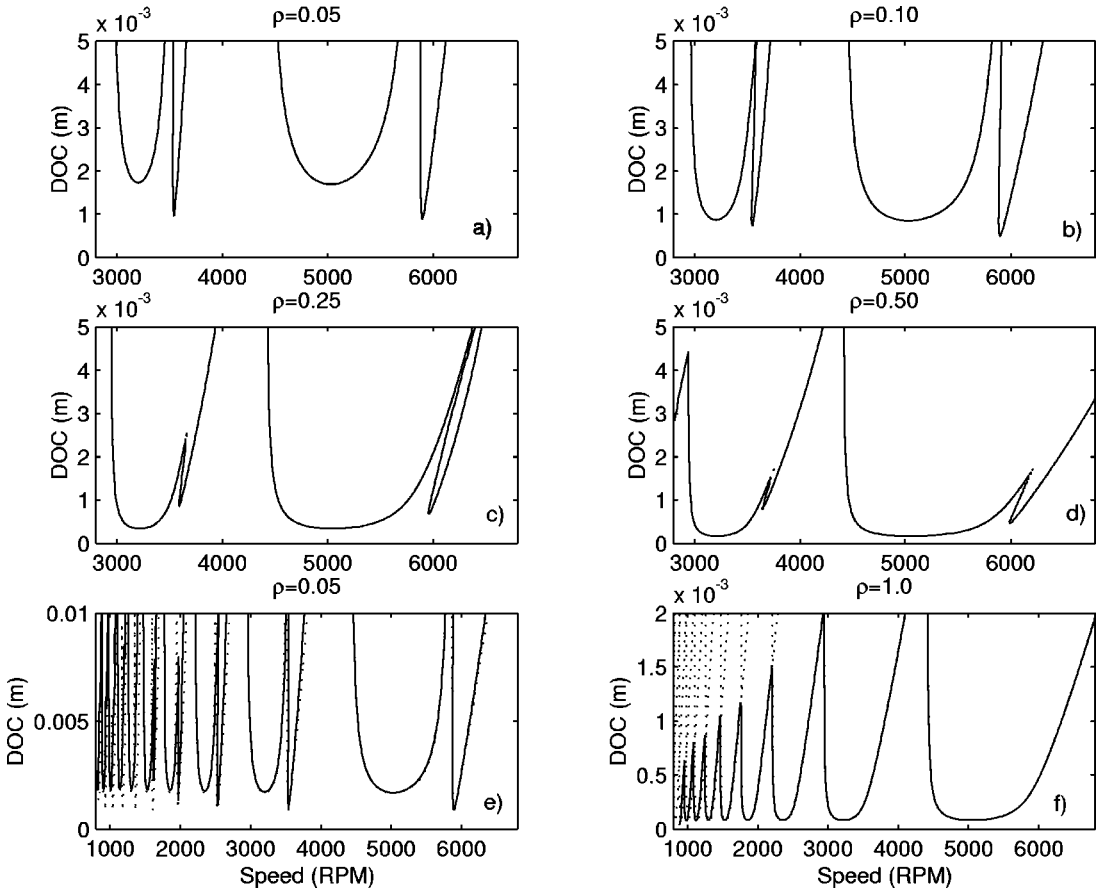

Fig. 2 Stability boundaries showing the effect of increasing the fraction of time in the cut (ρ). Parameters: $k=2.2\times10^6$ N/m, $f_n=146.8$ Hz, $\varsigma=0.0038$, $C=2.0\times10^8$ N/m^2. Number of elements: E=20ρ. Panel (e) shows a comparison of TFEA lobes with the stability lobes derived by the impulse approximation of Davies et al., 2000 (dotted lines). Panel (f) shows a comparison with stability lobes for continuous cutting derived by the method of Tlusty (1985) (dotted lines).

magnitude greater than 1. These routes are also found using the current method. As the time in the cut is increased, the number of elements is increased to maintain the same level of accuracy. There is no restriction on the time in the cut.

The current method is compared to the method of Davies et al. [5,6] for $\rho=0.05$ in Fig. 2(*e*). Agreement is very good at higher speeds, although the method of Davies et al. [5,6] loses accuracy at low speeds. As the wavelength of vibration becomes short, the force is less accurately modeled as an impulse. In Fig. 2(*f*), results for continuous cutting are compared with stability lobes obtained by the frequency domain method of Tlusty [12], e.g., which is exact for the continuous model.

Raw measurements and 1/rev samples of experimental data are shown in Fig. 3. Stable cuts are clearly indicated by a single steady-state value of the 1/rev samples. This distinguishes large-amplitude forced vibration (Fig. 3*a*,*b* e.g.) from chatter.

In Fig. 4, stability results from time-domain simulation and experiment are compared to the predicted boundaries. Cuts are designated as stable if 1/rev samples converge to a single steady value [13]. Agreement between numerical simulation and predictions is excellent (Fig. 4(*a*)). Agreement between experimental stability data (Fig. 4(*b*)) and analytical predictions is good. Both simulations and experiment confirm an increase in stability as depth of cut is increased from 1 to 5 mm (at ~3560 rpm in simulation, 3540 rpm in experiment). The experimental regions of instability are slightly smaller and shifted to the left, perhaps reflecting the omission of nonlinearity in cutting force, helix angle, and rotation of the cutting force vector.

Computation Time: Algorithms were implemented in MATLAB on a 233 MHz Pentium II PC with 288M RAM. The 50×10 grid of time-marching simulations ($\rho=0.1$) in Fig. 4(*a*) took 254 seconds; time finite element analysis (E=2) on the same grid took 0.96 seconds. For the higher resolution used in the figure a 200×50 grid was used, taking 19.6 seconds. The frequency domain analysis in Fig. 2(*f*) was completed in 1.73 seconds. The time finite element analysis ($\rho=1.0$, E=20, 200×20 grid) for the figure took 79.2 seconds. For small times in the cut, time finite element analysis is efficient and accurate; for full and near-full immersion, frequency domain analysis has the best combination of efficiency and accuracy.

4 Summary and Conclusions

In this paper we analyze a model of interrupted cutting with arbitrary time in the cut, via a set of discrete dynamic equations. The motion of the tool in the cut is governed by a delay-differential equation which incorporates the regenerative effect. The discrete-time equations are obtained by the use of temporal finite elements while the tool is in the cut. The approximate solution during the cut is required to match the exact solution for free vibration of the tool at the beginning and end of each cut. Eigenvalues of the discrete system with magnitude greater than one indicate instability.

Bounds on the depth of cut for stable cutting are found efficiently via this algorithm and are presented as a function of cutting speed. Experimental results confirm the general stability predictions of the discrete model. Results also confirm the qualitative

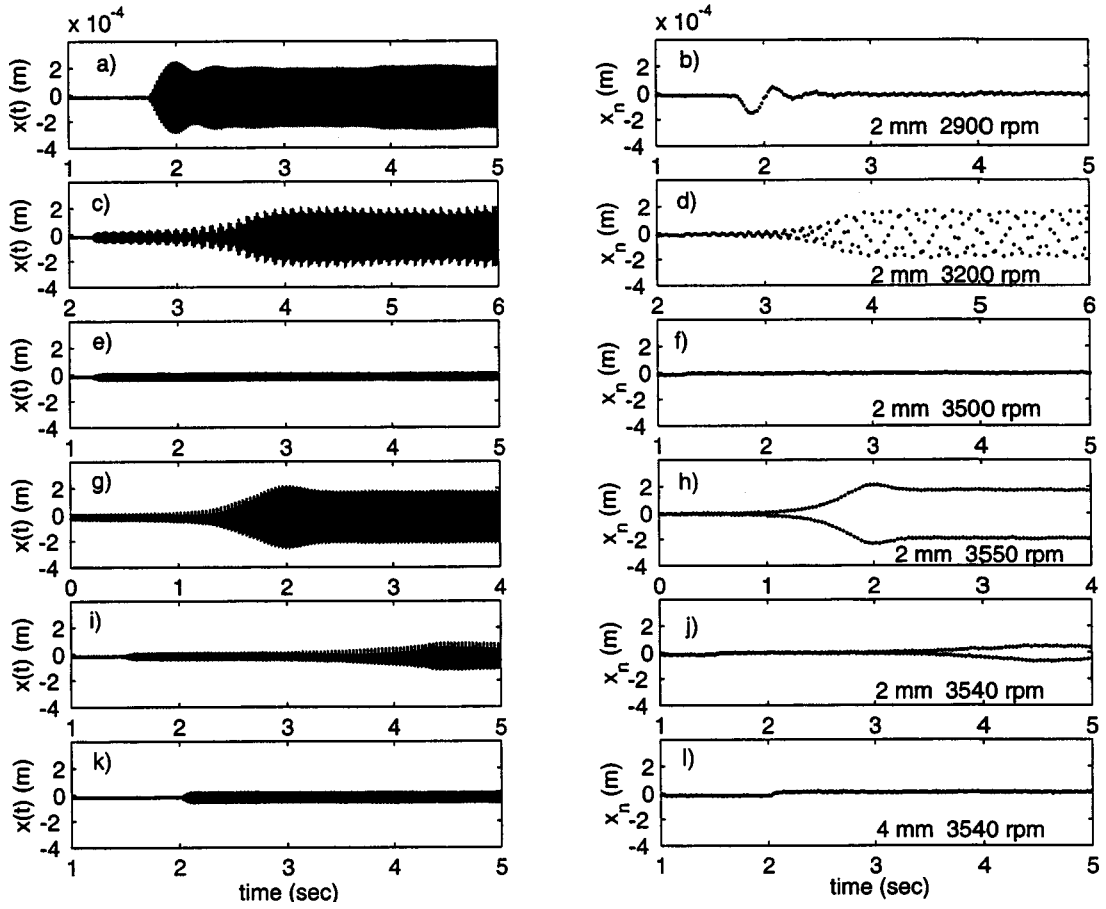

Fig. 3 Experimental data from continuous sampling (*a,c,e,g,i,k*) and 1/rev sampling (*b,d,f,h,j,l*) during milling of 1-DOF flexure. Parameters are as in Fig. 2; fraction of time in the cut $\rho = 0.1$. Row 1 (*a,b*): 2900 rpm, 2 mm DOC, stable; Row 2 (*c,d*): 3200 rpm, 2 mm DOC, unstable; Row 3 (*e,f*): 3500 rpm, 2 mm DOC, stable; Row 4 (*g,h*): 3550 rpm, 2 mm DOC, unstable; Row 5 (*i,j*): 3540 rpm, 2 mm DOC, unstable; Row 6 (*k,l*): 3540 rpm, 4 mm DOC, stable.

predictions of Davies et al. [5,6] of additional stability regions. In particular, a prediction of this model was confirmed in tests when stability was obtained at 3540 rpm by *increasing* the depth of cut from 1 mm to 5 mm.

In planned future work, the current approach can be refined to better describe the process of milling. Directional variation of cutting force, more modes, and more degrees of freedom may be included. The use of time finite elements is a powerful and flexible approach to the solution of equations with periodic coefficients and time-delays.

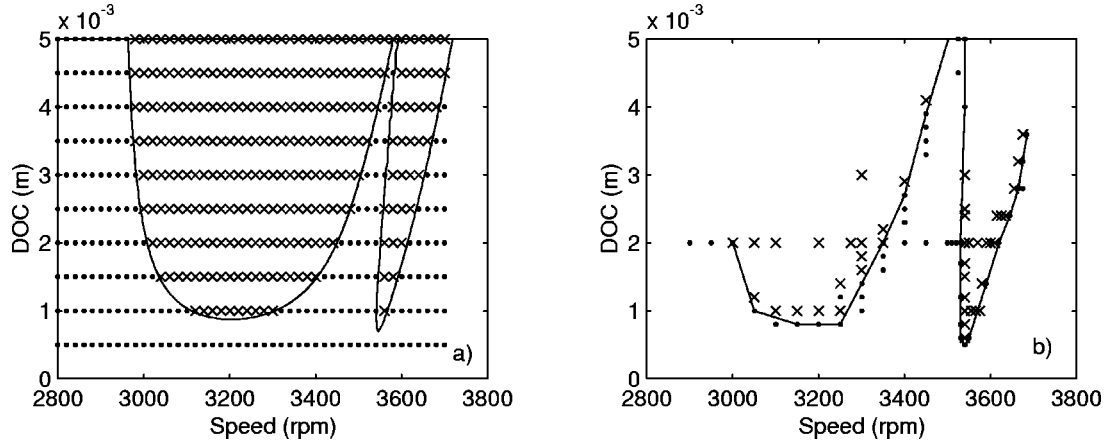

Fig. 4 Comparison of (*a*) predicted stability boundaries (lines) with results from simulation (· stable, x unstable); (*b*) experimental data (· stable, x unstable). Parameters are as in Fig. 2; fraction of time in the cut $\rho = 0.1$. Note that in experimental cutting tests at 3540 rpm a DOC of 5 mm is stable and a DOC of 1 mm, for example, is unstable. Analogous behavior is predicted by analysis and observed in simulation.

Acknowledgments

We gratefully acknowledge support from the Boeing Company and the National Science Foundation Grants DMI-9900108 (GOALI) and CMS-9625161 (CAREER). David A. Peters provided guidance in the application of time finite elements. Wendy Shefelbine and Ryan Hanks contributed valuable assistance.

References

[1] Koenigsberger, F., and Tlusty, J., 1970, *Structures of Machine Tools*, Pergamon Press, Oxford.
[2] Tobias, S. A, 1965, *Machine Tool Vibration*, Wiley, New York.
[3] Smith, S., and Tlusty, J., 1991, ''An Overview of the Modeling and Simulation of the Milling Process,'' ASME J. Eng. Ind., **113**, pp. 169–175.
[4] Altintas, Y., and Budak, E., 1995, ''Analytical Prediction of Stability Lobes in Milling,'' CIRP Ann., **44**, pp. 357–362.
[5] Davies, M. A., Pratt, J. R., Dutterer, B., and Burns, T. J., 2001, ''Interrupted Machining: A Doubling in the Number of Stability Lobes,'' ASME J. Manuf. Sci. Eng., **124**, pp. 217–225.
[6] Davies, M. A., Pratt, J. R., Dutterer, B., and Burns, T. J., 2000, ''The Stability of Low Radial Immersion Machining,'' CIRP Ann., **49**, pp. 37–40.
[7] Corpus, W. T., and Endres, W. J., 2000, ''A High-Order Solution for the Added Stability Lobes in Intermittent Machining,'' *ASME Publication MED-Vol. 11, Proceedings of the ASME Manufacturing Engineering Division*, pp. 871–878.
[8] Insperger, T., and Stepan, G., 2000, ''Stability of the Milling Process,'' Periodica Polytechnica Ser. Mech. Eng., **44**, pp. 47–57.
[9] Bayly, P. V., Halley, J. E., Davies, M. A., and Pratt, J. R., 2000, ''Stability Analysis of Interrupted Cutting with Finite Time in the Cut,'' *ASME Publication MED-Vol. 11, Proceedings of the ASME Manufacturing Engineering Division*, pp. 989–996.
[10] Peters, D. A., and Idzapanah, A. P., 1988, ''hp-Version Finite Elements for the Space-Time Domain,'' Computational Mechanics, **3**, pp. 73–88.
[11] Meirovitch, L., 1997, *Principles and Techniques of Vibrations*, pp. 544–548, Prentice Hall, New Jersey.
[12] Tlusty, J., 1985, ''Machine Dynamics,'' *Handbook of High-Speed Machining Technology*, R. I. King, ed., Chapman and Hall, New York.
[13] Schmitz, T. L., Davies, M. A., Medicus, K., and Snyder, J., 2001, ''Improving High-Speed Machining Material Removal Rates by Rapid Dynamic Analysis,'' CIRP Ann., **50**, pp. 263–268.